Manifestation of quantum chaos in Fano-Feshbach resonances

Lucie D. Augustovičová and John L. Bohn

Phys. Rev. A **98**, 023419 — Published 20 August 2018

DOI: 10.1103/PhysRevA.98.023419

Manifestation of Quantum Chaos in Fano-Feshbach Resonances

Lucie D. Augustovičová[1] and John L. Bohn[2]
[1] *Charles University, Faculty of Mathematics and Physics, Department of Chemical Physics and Optics, Ke Karlovu 3, CZ-12116 Prague 2, Czech Republic and*
[2] *JILA, NIST, and Department of Physics, University of Colorado, Boulder, CO 80309-0440, USA*

A model is presented that mimics the nearest-neighbor-spacing (NNS) distribution of chaotic molecules such as Dy_2 and Er_2 just below their dissociation threshold. In this model the degree of chaos is controlled by choosing suitable Hamiltonian matrices from random ensembles. It is found that, in versions of the model that are not completely chaotic, the NNS of observable Fano-Feshbach resonances exhibits greater level repulsion, hence more chaos, than the corresponding NNS of a typical energy spectrum of the molecule at a fixed magnetic field.

PACS numbers:

I. INTRODUCTION

Recently, evidence of quantum chaos has been reported in ultracold collisions of both erbium and dysprosium atoms [1–5]. The states contributing to chaotic spectra are those that lie immediately below the dissociation threshold of the Dy_2 or Er_2 molecule. This is unusual: chaos is predicted to be present in triatomic systems at or just below dissociation, such as Ar_3 clusters [6], as well as ultracold collisions of Li+CaH [7] or Rb+K_2. However, it is less obvious that diatomic molecules could present chaotic behavior.

The observation of chaos in Dy_2 and Er_2 was assisted by the circumstance of extremely low temperatures, on the order of hundreds nK. This circumstance enabled high-resolution spectroscopy of distinct states, which revealed quantum chaos by the usual measures of nearest-neighbor-spacing statistics or spectral rigidity.

There is, however, a novelty in the observations of Refs. [1–5], at least from the point of view of quantum chaos. The resonant states were observed as a function of magnetic field, rather than as a function of energy, as would be the case in conventional spectroscopy. This is a very natural consequence of spectroscopy in ultracold gases, where the energy of a pair of colliding atoms is fixed – essentially at zero – while the resonant states can be moved, in this case by means of the magnetic field, through this energy, where they are observed as $E = 0$ scattering resonances.

The spectra of the near-dissociation molecules generally appear as in Figure 1. This figure is the result of a schematic model of Dy_2 energy levels, to be described in Sec. II. The point here is that, at each value of the magnetic field B, there exists a spectrum of bound state energies that may exhibit some degree of quantum chaos. As the magnetic field is increased, this spectrum evolves, in such a way that the energy states move closer to, and eventually cross, the dissociation threshold, taken here to be $E = 0$. This threshold corresponds to the lowest-energy states of a pair of free atoms, each in the $|jm\rangle = |8, -8\rangle$ state in this case. At each magnetic field where one of these bound state crosses the threshold, a scattering resonance appears, which is observed by means of the excessive three-body recombination that accompanies it. The resulting set of magnetic field values constitutes a spectrum, which can be analyzed by means of the usual tools of quantum chaos.

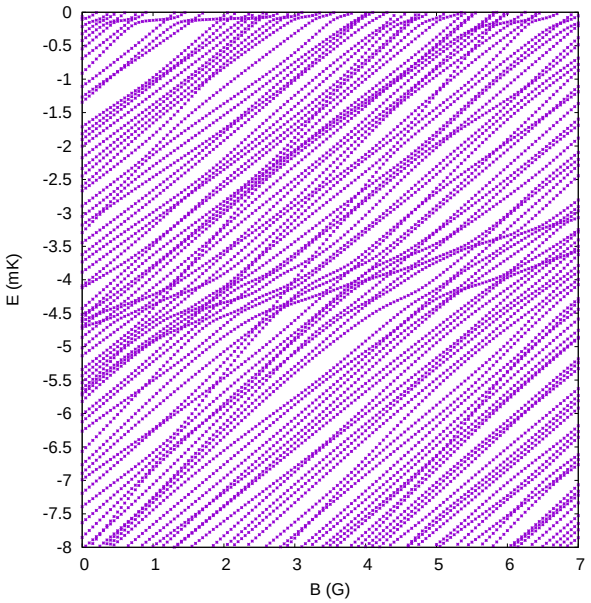

FIG. 1: Simulated spectrum of Dy_2 molecules, versus magnetic field, generated as described in the text. Each energy level at $B = 0$ evolves as the magnetic field is increased, eventually finding its way to zero energy, where it appears as a scattering resonance.

The measured spectra of Dy_2 and Er_2 are therefore unusual, inasmuch as they consist of magnetic field values, rather than energies. What is recovered is not the energy spectrum of a chaotic molecule, but rather a spectrum consisting of a *single* energy level from each of *many different* chaotic molecules, since the molecular Hamiltonian giving rise to these bound states is different for each magnetic field.

This distinction raises questions regarding the interpretation of the measurement. If chaos is found in the

spectra of magnetic field values, does it imply the same degree of chaos would be found in the energy spectrum at any fixed magnetic field? If not, which is "more chaotic," and how do we quantify the difference?

In this article we make a preliminary investigation into these questions. In Section II we construct a fairly realistic model of Dy_2 molecules and extract from it spectra of energies at constant magnetic field, and spectra of magnetic field values at constant energy. These spectra are analyzed in terms of their nearest-neighbor-spacing (NNS) and quantified by the free parameters of their respective Brody distribution [8]. It is found that both spectra yield Brody parameters near unity, i.e., that both the energy and magnetic field spectra are fully chaotic.

In Sec. III we introduce a family of extended models in such a way that effective channel couplings in the molecule can be reduced, making the molecules less chaotic. We find that for any given member of this family that is not completely chaotic, the Brody parameter of the magnetic field spectrum is generally greater than that for the energy spectrum, $\nu_B > \nu_E$, implying that the magnetic field spectrum may exhibit a greater degree of chaos. In Section III we also simplify the model further to garner insight into why this might be so. We conclude in Section IV.

II. MODEL OF THE DIATOMIC SPECTRA

We begin with a simplified model of these molecules, which incorporates features of about the right quality and scale. It is a simplified version of a complete scattering calculation carried out by [1]. The essence of this approximate calculation is to separate the basic structure of ro-vibrational energy levels, and spins, from the strong anisotropic couplings that ultimately generate the chaos.

A. Hamiltonian

This model describes a pair of ^{162}Dy atoms in their ground state with spin $j = 8$ and g-factor $g = 1.2508$ [9]. The nuclear spin of these atoms is zero. (A similar model can be constructed for Er, of course). The model Hamiltonian is taken to be

$$H = H_{\rm rv} + H_{\rm mag} + V_{\rm an}. \tag{1}$$

Briefly, $H_{\rm rv}$ describes the ro-vibrational degrees of freedom, $H_{\rm mag}$ their shifts in a magnetic field, and $V_{\rm an}$ the coupling of these states due to the anisotropic potential energy surface. V is regarded as the part that engenders chaos in the spectra.

In more detail: We begin with a Lennard-Jones potential that describes an approximately correct long-range interaction between the atoms, so that the spacing of ro-vibrational levels is realistic. This potential, including a centrifugal potential, is

$$V_{\rm LJ} = \frac{C_{12}}{R^{12}} - \frac{C_6}{R^6} + \frac{\hbar^2 L(L+1)}{2\mu R^2}, \tag{2}$$

where R is the distance between the atoms, μ the reduced mass of the atom pair, and $C_6 = 2\,003$ au [1] is the isotropic van der Waals coefficient of Dy_2. C_{12} is chosen so that the depth of the potential is set to 785.7 $\rm cm^{-1}$ [10].

From this potential, a set of radial basis functions $|L, v\rangle = \phi_{L,v}(R)$ is numerically constructed as eigenfunctions of $H_{\rm rv}$,

$$-\frac{\hbar^2}{2\mu}\frac{d^2\phi_{L,v}}{dR^2} + V_{\rm LJ}\phi_{L,v} = E_{L,v}\phi_{L,v}. \tag{3}$$

Taken together with the spins of the two atoms and the partial wave angular momentum, these states define the basis of this model,

$$|L, v\rangle|LM_L\rangle|j_1 m_1\rangle|j_2 m_2\rangle. \tag{4}$$

Further, in this basis the magnetic field Hamiltonian is diagonal, with energies given by

$$H_{\rm mag}|j_1 m_1\rangle|j_2 m_2\rangle = g\mu_B(m_1 + m_2)B\,|j_1 m_1\rangle|j_2 m_2\rangle, \tag{5}$$

where μ_B is the Bohr magneton.

The observations occur upon scattering atoms in their ground state, $|jm\rangle = |8, -8\rangle$ at ultracold temperatures, whereby the initial partial wave angular momentum is $L = 0$. Starting from this state, we consider all basis states (4) consistent with conservation of angular momentum and boson exchange symmetry. Moreover, we consider the energy of two free atoms in the $|8, -8\rangle$ state to define the zero of energy at all values of magnetic field. As a consequence, the energies of the basis states in (4) have the magnetic field dependence

$$E_{L,v} + g\mu_B\Big[(m_1 + 8) + (m_2 + 8)\Big]B. \tag{6}$$

This ensures that the energies of all the bound states are rising functions of magnetic field, and that the magnetic field spectrum will be identified with these levels crossing $E = 0$. These energies are more-or-less independent from one potential to the next, and ensure a random, non-chaotic spectrum, characterized by a nearest-neighbor distribution having Poisson statistics.

To generate chaos in such a spectrum requires strong off-diagonal coupling, represented here by $V_{\rm an}$. This potential can contain the magnetic dipole-dipole interaction between the atoms,

$$V_{\rm dd}(\vec{R}) = -\left(\frac{g\alpha}{2}\right)^2 \frac{3\,(\hat{R}\cdot\vec{j_1})(\hat{R}\cdot\vec{j_2}) - \vec{j_1}\cdot\vec{j_2}}{R^3}, \tag{7}$$

where α is the fine structure constant; and an anisotropic dispersion interaction

$$V_{\rm ad}(\vec{R}) = -\frac{C_{ad}}{\sqrt{6}}\sum_{i=1}^{2}\frac{3\,(\hat{R}\cdot\vec{j_i})(\hat{R}\cdot\vec{j_i}) - \vec{j_i}\cdot\vec{j_i}}{R^6}. \tag{8}$$

Here $\vec{R} = R\hat{R}$ is the interatomic separation vector in relative coordinates. It has been observed previously that $V_{\rm dd}$ is primarily responsible for anisotropic coupling in Dy_2, while $V_{\rm ad}$ is more important for Er_2 [1, 11].

In the basis (4) these interactions have the matrix elements

$$\langle L'v'|\langle L'M'_L|\langle j_1m'_1|\langle j_2m'_2|V_{\rm an}|L,v\rangle|LM_L\rangle|j_1m_1\rangle|j_2m_2\rangle = \sum_{q=-2}^{2}(-1)^{q+1}\langle L'M'_L|C_{2q}|LM_L\rangle\Big\{\sqrt{6}\left(\frac{g\alpha}{2}\right)^2\times \langle L'v'|\frac{1}{R^3}|L,v\rangle\langle j_1m'_1|\langle j_2m'_2|(j_1\otimes j_2)_{2,-q}|j_1m_1\rangle|j_2m_2\rangle + C_{\rm ad}\langle L'v'|\frac{1}{R^6}|L,v\rangle\times \langle j_1m'_1|\langle j_2m'_2|(j_1\otimes j_1)_{2,-q}+(j_2\otimes j_2)_{2,-q}|j_1m_1\rangle|j_2m_2\rangle\Big\}, \quad (9)$$

where $(j_1\otimes j_2)_{2,-q}$ is the $-q$-component of the compound irreducible second rank tensor product of tensors of rank 1 (vectors) that act as the total angular momentum operators on the individual variables in spaces 1 and 2. C_{kq} is the modified spherical harmonic. The value of $C_{\rm ad} = 0.168\ E_{\rm h}a_0^6$ [10].

B. Spectrum and chaos

Thus the Hamiltonian matrix can be constructed and diagonalized for any desired value of magnetic field B. The resulting map of eigenenergies versus B is shown in Figure 1. To achieve this figure, 7103 basis functions having their partial-wave function of even L up to $L_{\rm max} = 28$ were needed to reach convergence of eigenstates of H. The energies change substantially for $L_{\rm max} < 22$, but in turn as $L_{\rm max}$ increases their positions converge and for $L_{\rm max} = 28$ they do not deviate from their converged values by more than 8×10^{-6} K in the range of energy shown.

This spectrum shows several remarkable features. Mainly, it consists of a collection of nearly-parallel curves, with occasional avoided crossings. The mean slope of these lines is approximately 1 mK/G, corresponding to about $15\mu_B$. This is comparable to the mean value of all the bare magnetic moments described by (6), whose average value would be $20\mu_B$ if all values of m were equally likely. The point is that strong interchannel couplings in this case lead to a remarkably uniform set of magnetic moments for all states. If the lines in Figure 1 were all straight lines with the same slope, then the magnetic field spectrum at $E = 0$ would be a faithfully rescaled copy of the energy spectrum at $B = 0$, and the two spectra would exhibit exactly the same degree of chaos. That these curves are not perfectly parallel is the first hint that the chaos in the two spectra may not be equivalent.

In addition, several lines in Figure 1 have a considerably smaller slope. These are likely due to broad "halo" resonances tied to the incident channel as were discovered in Ref. [12] and that are expected to persist across many narrower, chaotic lines in the spectrum. While such states are interesting, they are in the minority and do not significantly affect the conclusions we draw here.

We seek to quantify the degree of chaos present in the two kinds of spectra: one, an energy spectrum at a fixed value of B; and the other, a magnetic field spectrum at $E = 0$. To do so, we employ the basic tool widely used for this purpose, namely, we fit the nearest-neighbor spacing (NNS) distribution [8], normalized so that the mean NNS is equal to one. As is conventional, we then fit this distribution to the Brody function:

$$P(\nu,s) = (1+\nu)\alpha s^{\nu}\exp(-\alpha s^{\nu+1}), \quad (10)$$

where $\alpha = [\Gamma((\nu+2)/(\nu+1))]^{\nu+1}$, s is the normalized NNS, and ν is the Brody parameter. This parameter is considered to be a measure of the chaos on the spectrum: $\nu = 0$ corresponds to a random, non-chaotic, Poisson spectrum, while $\nu = 1$ corresponds to a fully chaotic spectrum whose levels are chaotic and characteristic of the eigenvalues of matrices from the Gaussian orthogonal ensemble (GOE). We will extract two kinds of Brody parameters, ν_E for a spectrum of energy values, and ν_B for a spectrum of magnetic field values.

The NNS and the Brody parameter represent only one approach to quantifying chaos in a quantum mechanical system. The methods of statistical analysis of spectra are many and diverse, and subsequent analyses have looked more deeply at the experimental spectra. Reference [13] analyzed the original Er data set in [2], finding that the NNS distribution is likely to underestimate the degree of chaos if levels are missing from the spectra, that is, if they are too narrow to be observed. This is shown by an analysis of the power spectrum of long-range correlations in far apart spectral levels [14] as well as by analyzing the distribution of resonance widths in comparison with the Porter-Thomas distribution. This analysis is consistent with the data if all resonances narrower than ~ 10 mG are unobserved, which amounts to about 20% of them. The suggestion was that the spectrum was indeed chaotic, but the resolution of the data were not yet sufficient to draw this conclusion. The analysis is further complicated by the sensitive temperature dependence of observable effects of the resonances [1].

Nevertheless, in our theoretical study we are able to resolve all resonances and use the Brody parameter exclusively as a measure of chaos. In Figure 2 are shown two histograms of the data in Figure 1. Fig. 2a) is drawn from the $B = 0$, energy spectrum, and yields a Brody parameter $\nu_E = 1^{+0}_{-0.23}$. Fig. 2b) is drawn from the $E = 0$, magnetic field spectrum, and yields $\nu_B = 0.93^{+0.07}_{-0.28}$. In both cases, the histograms are generated from 250 levels of the spectrum. The uncertainties are the 1-σ uncertainties due to the fit to the Brody function (10). This uncertainty arises due to the counting statistics of data in the histogram. It is compelling to assert that both these spectra are "fairly chaotic," and that therefore chaos is

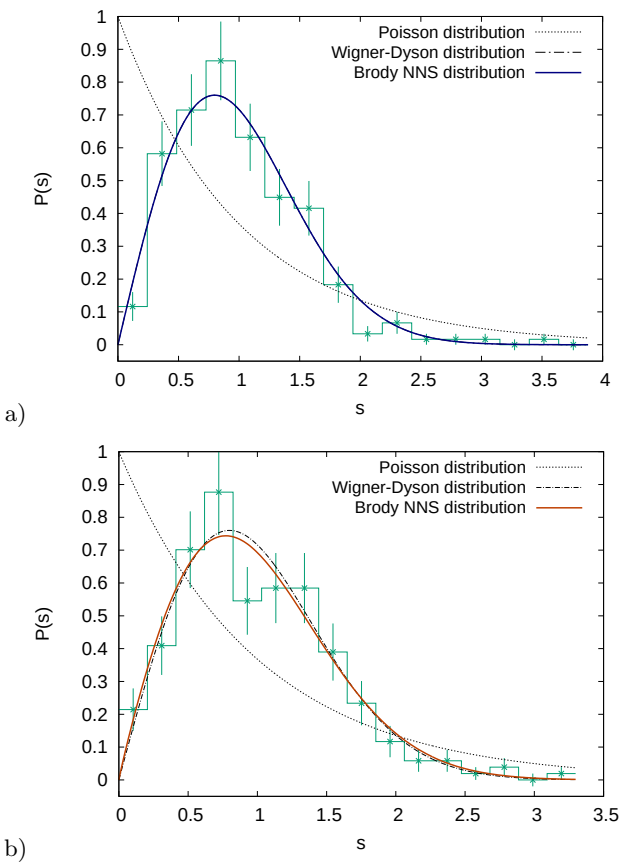

FIG. 2: Nearest-neighbor spacing (NNS) distributions for the spectrum shown in Figure 1. In a) is shown the $B = 0$ spectrum, while in b) is shown the $E = 0$ spectrum.

preserved in the mapping from energy spectra to magnetic field spectra. However, the large fit uncertainties make a quantitative statement difficult. With these uncertainties, the value of ν_B is somewhat higher than, but nearly consistent with, the values $\sim 0.5 - 0.75$ extracted from the original ^{164}Dy data [1].

C. Simulation of lesser-strength anisotropy

In order to beat down the large error bars associated to a single statistical evaluation of the spectra ensemble we exploit the theory of random matrices. The nonzero matrix elements of $V_{\rm an}$ for a chaotic molecule are viewed as random variables distributed around zero with a variance w_0. This allows us to simulate the molecule more generically by using the matrix elements distributed according to the probability densities [15]

$$P(w, V_{ii}) = \frac{1}{\sqrt{2\pi}w} \exp\left(-\frac{V_{ii}^2}{2w^2}\right),$$
$$P(w, V_{ij}) = \frac{1}{\sqrt{\pi}w} \exp\left(-\frac{V_{ij}^2}{w^2}\right), \quad i \neq j. \qquad (11)$$

To approximate the Dy_2 model given in the previous section, we set the width w to the root-mean-squared width determined from the nonzero matrix elements computed above. This width is $w_0 = 24.7$ mK.

The interaction matrix is constructed by filling those elements that are not zero by symmetry with random variables determined from the GOE distributions (11), while treating the diagonal elements of $H_{\rm rv}$ and $H_{\rm mag}$ as before. In this way we can generate many realizations of models of Dy_2 and find an ensemble of independent Brody parameters that can be averaged to reduce the collective uncertainty of the set. Approximately 30 such realizations are required to reduce the uncertainty to 5%. The resulting Brody parameters are then $\nu_E = 0.94 \pm 0.05$, and $\nu_B = 0.98 \pm 0.05$, respectively. We conclude that our basic model of Dy_2 is fully chaotic, and is equally chaotic in energy and magnetic field spectra.

The random matrix version of the theory affords also the opportunity to turn off the chaos in a controlled way. Namely, as the value of w is reduced, the magnitudes of the matrix elements of $V_{\rm an}$ are reduced, generating less level repulsion in the eigenvalues of H, and bringing the spectrum closer to the essentially random spectrum of $H_{\rm rv} + H_{\rm mag}$. That is, the Brody parameters are generally expected to be increasing functions of w. We refer to such a model, with less chaos than a more realistic dysprosium model, as the "sub-dysprosium" model.

We note that a similar model was described in Ref. [1]. There are some significant differences, however. Ref. [1] distributed the magnetic moments randomly and, more significantly, allowed the diagonal spectrum to have its own Brody parameter, independent of the size of random off-diagonal matrix elements. A main conclusion from that calculation was that the Brody parameter of the magnetic field resonance spectrum rose as a function of channel coupling just the same, regardless of the original diagonal Brody parameter. This was strong evidence that the chaos in the observed spectra lay in the avoided crossings in figures such as Fig. 3d of Ref. [1], or Fig. 1 of this paper. Reference [1] did not, however, make a direct comparison between energy and magnetic field spectra for a given channel coupling, as we do here.

For our model, the resulting parameters ν_E for magnetic field $B = 10$ G (for reasons explained below) and ν_B for energy $E = 0$ are shown versus w in Figure 3. For full strength of anisotropic coupling, $w = w_0$, both spectra have essentially unit Brody parameters are and both fully chaotic, and agree with the results of the model in the previous section (solid points). Both Brody parameters drop rapidly as w decreases, but ν_E drops much more rapidly. Therefore, for a given version of sub-dysprosium that is not completely chaotic, the magnetic field spectrum of Fano-Feshbach resonances would appear more chaotic than would the energy spectrum at a given magnetic field. For much smaller values of w the spectra both return to random, Poisson-like NNS, and do not differ as dramatically.

A caveat in preparing this Figure 3 is that the energy

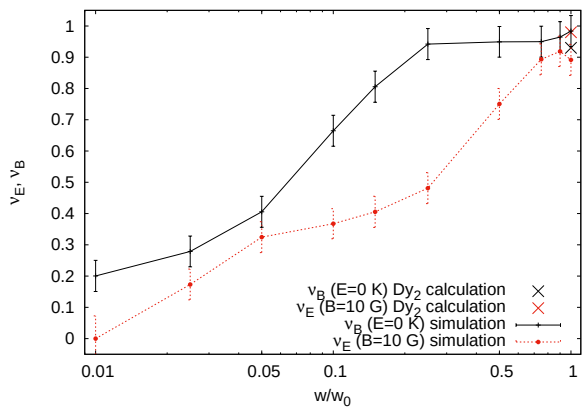

FIG. 3: Brody parameters ν_E and ν_B for the simulation of 'sub-Dysprosium' as a function of the width parameter w in the units of $w_0 = 24.7$ mK, and for Dy_2 calculation (shown in Figure 1) evaluated from discrete energy values for $B = 10$ G [red (dark gray) cross at $0.98^{+0.02}_{-0.25}$], and from resonance positions at $E = 0$ K [black cross at $0.93^{+0.07}_{-0.28}$]. Error bars for values at large crosses are not shown.

spectrum is computed at a magnetic field $B = 10$ G, rather than $B = 0$. This is because, for small B, the spectrum has two characteristic energy scales. There is a small energy scale given by the very regular spacing of Zeeman levels; and a larger energy spacing given by the characteristic ro-vibrational energies. This leads to a bimodal NNS that is not well described by a Brody distribution for any value of ν_E. Once a field is applied and Zeeman energy splitting become comparable to ro-vibrational splittings, this is no longer an issue.

III. SCHEMATIC MODEL OF MAGNETIC-FIELD DEPENDENCE

Examination of the onset of chaos in sub-dysprosium in Figure 3 suggests that the Brody parameter curves $\nu_E(w)$ and $\nu_B(w)$ have the same shape, namely, a sigmoidal dependence that rises first then saturates at unity. The two curves can be made to nearly overlap by shifting one of them along the logarithmic w axis. Another way to say this is that for a given value of w in the model, the two kinds of spectra have different *effective* values of w, scaled by some factor. In this section we explore this idea.

To do so, it is worthwhile to construct an even simpler model that incorporates the essential features of the sub-dysprosium model, but that lends itself better to analytical understanding. These essential features are: an underlying spectrum of pseudo-vibrational states representing the molecule in zero field; a collection of pseudo-magnetic moments that map these energies to magnetic field values; and a strong mixing that generates chaos.

A. It's Only a Model

To this end, we contemplate a set of N_v energy levels, E_i, to represent the $B = 0$ molecule. These energies have mean spacing E_0, which defines the unit of energy. They are chosen randomly in the energy interval $[-N_v E_0, 0]$, appropriate to pseudo-vibrational states lying below a threshold at $E = 0$. Each of these is assumed to have a d-fold degeneracy of pseudo-magnetic levels, bringing the total number of states in the model to $N = N_v d$. These degenerate states are enumerated by pseudo-magnetic quantum numbers, $m = 1, 2, \ldots d$. The degeneracy of these states is lifted in a magnetic field, which each one getting an additional energy $m\mu B$, which represents all the states rising in energy with magnetic field. The combination μB effectively defines the magnetic field unit $B_0 = E_0/\mu$.

The Hamiltonian of the model is then given in matrix form as

$$H_{\rm schematic} = D + V + \mu B M, \tag{12}$$

where D and M are diagonal matrices,

$$D = {\rm diag}(E_1, E_1, \ldots, E_1, E_2, E_2, \ldots, E_2, \ldots, E_{N_v}), \tag{13}$$

where each energy E_i is repeated d times; and

$$M = {\rm diag}(1, 2, \ldots d, 1, 2, \ldots, d, \ldots, d). \tag{14}$$

In this way, all the original pseudo-vibrational levels move to intercept the $E = 0$ axis somewhere in the interval $B \in [0, N_v E_0/\mu]$, see Figure 4a. The energy and magnetic field spectra are therefore characterized by mean spacing of, respectively,

$$\begin{aligned} \Delta E &= \frac{N_v E_0}{N_v d} = \frac{E_0}{d} \\ \Delta B &= \frac{E_0/\mu}{d}. \end{aligned} \tag{15}$$

Chaos is introduced into the model via the coupling matrix V, in the same way it was for the sub-dysprosium model. That is, the elements of V will be drawn from the Gaussian orthogonal ensemble given in (11). Sample spectra for $w = 0.8\ E_0$ are shown in Figure 4b. These spectra reproduce, at least qualitatively, the features of the more realistic model in Figure 1. Note especially that the lines are nearly, but not quite, parallel, representing the regularization of magnetic moments of all the states.

B. Chaos in the Model

Using this schematic model, we compute the Brody parameters $\nu_E(w)$ and $\nu_B(w)$ as functions of w, and for several different values of spin degeneracy d. The results are shown in Figure 5. In general all curves show the familiar sigmoidal dependence that shows how the chaos turns on as w is increased.

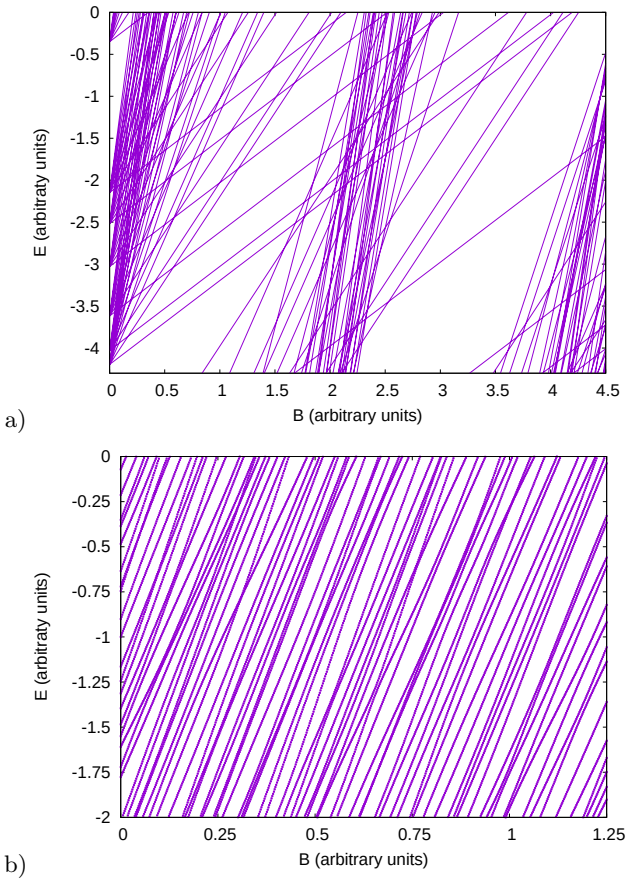

FIG. 4: Simulated spectra for the schematic model of chaotic molecules in a magnetic field in the case of 10-fold degeneracy. In a) is shown the non-chaotic version, $w = 0$, illustrating the movement of levels from the energy axis to the magnetic field axis. In b) is shown a chaotic spectrum with $w = 0.8$; compare to Figure 1.

The specific curves are different, however. In general, larger spin degeneracies d cause the curves $\nu_E(w)$ and $\nu_B(w)$ to shift to smaller values of w, indicating an earlier onset of chaos. Moreover, for a given value of $d > 1$, ν_B is shifted to smaller w than ν_E, as in the sub-dysprosium model, suggesting that for a given model with a given value of w, the magnetic field spectrum exhibits a greater degree of chaos by this measure. For $d = 1$, the two Brody parameters coincide.

Qualitatively, these features can be understood in simple terms. For example, in the energy spectra the mean energy spacing is $\Delta E = E_0/d$. The spectrum, random when $w = 0$, starts to see significant mixing and level repulsion when off-diagonal matrix elements in the Hamiltonian, of order w, become comparable to the mean spacing of the diagonal elements. Thus for $d = 1$ the transition to chaos is nearly complete when $w = 1$ (recall that w is given in units of E_0 in the plot). But for larger values of d, the coupling w should be compared to a smaller mean spacing E_0/d, so that the level repulsion, hence chaos, appears at smaller values of $w \sim E_0/d$. Thus the

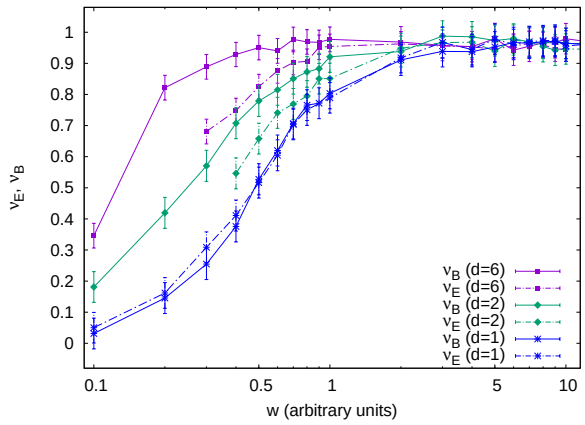

FIG. 5: Brody parameters ν_E and ν_B for the schematic model presented in Sec. II.A, as a function of the width parameter w.

Brody parameters ν_E (dashed curves in Figure 5) are shifted leftward in the figure for larger d.

Similarly, for a given degeneracy d, the magnetic field spectrum becomes chaotic for smaller w than does the corresponding energy spectrum. This suggests that the magnetic field spectrum possesses a larger ratio of effective coupling to mean level spacing, at least in the range explored, than does the energy spectrum. We can see this as follows.

To find the $B = 0$, energy spectrum, we solve the matrix diagonalization

$$(D + V)x^{(\alpha)} = e_\alpha x^{(\alpha)} \tag{16}$$

for the energy eigenvalues e_α and eigenstates $x^{(\alpha)}$. The size of w in the matrix V, as compared to the mean spacing ΔE of the diagonal elements of D, controls the degree of chaos and the value of the Brody parameter.

Similarly, the $E = 0$, magnetic field spectrum is given by setting the energy to zero, thereby solving

$$(D + V + \mu BM)y = 0 \tag{17}$$

for the spectrum of B values. Since M is a positive definite matrix, $M^{1/2}$ and $M^{-1/2}$ exist, and this matrix equation is equivalent to the diagonalization

$$(\tilde{D} + \tilde{V})\tilde{y}^{(\alpha)} = b_\alpha \tilde{y}^{(\alpha)}, \tag{18}$$

where the transformed matrices, in units of magnetic field, read

$$\begin{aligned} \tilde{D} &= -\frac{1}{\mu} M^{-1/2} D M^{-1/2} \\ \tilde{V} &= -\frac{1}{\mu} M^{-1/2} V M^{-1/2}, \end{aligned} \tag{19}$$

and the eigenstate is changed to

$$\tilde{y} = M^{1/2} y. \tag{20}$$

The magnetic field spectrum derives from a qualitatively different eigenvalue problem (18) than the one in Eqn. (17) that gives the energy spectrum. For one thing, the unperturbed spectrum (diagonal elements of $\tilde{D}$) no longer have a uniform density of states. To see this, note that the diagonal elements of $\tilde{D}$ have the form $B_i = -E_i/(m\mu)$. Thus the spectrum is squeezed to smaller values of B for larger values of m, as can be seen in Figure 4a. The small region of magnetic field in the interval $B \in [0, N_v B_0/d]$, contains a number of states given by

$$\sum_{m=1}^{d} \frac{N_v}{d} m = \frac{N_v}{d} \frac{d(d+1)}{2}. \tag{21}$$

The density of states in this near-zero-field interval is then

$$\rho_B = \frac{d(d+1)}{2B_0}. \tag{22}$$

This is higher than the value d/B_0 given by taking the total number and dividing by the total magnetic field range. It is worthwhile to restrict attention to this magnetic field region where the density of states is relatively uniform. Such a region can cover as many magnetic field resonance values as desired, by simply increasing N_v.

Similarly, the matrix $\tilde{V}$ is no longer necessarily drawn from the GOE, since its matrix elements become $-V_{ij}/(\mu\sqrt{mm'})$, and are diminished by the m quantum numbers of the states involved. In this case the matrix element distributions no longer share a common width as implied by (11). Rather, for each given pair of numbers m, m', the matrix elements V_{ij} are Gaussian distributed, with an effective width $w_{mm'} = w/(\mu\sqrt{mm'})$.

The net distribution of all matrix elements will no longer be Gaussian, in general, but for the sake of approximation we can define a Gaussian distribution whose width is defined by the root-mean-square deviation of the matrix elements. That is, given the mean squared width $\langle V_{ij}^2 \rangle = w^2/2$, the mean squared width of any off-diagonal element of $\tilde{V}$ is

$$\begin{aligned} \frac{\tilde{w}^2}{2} &= \frac{1}{d^2} \sum_m \sum_{m'} \frac{w^2}{2\mu^2} \frac{1}{mm'} \\ &= \frac{w^2}{2\mu^2} \frac{1}{d^2} \left(\sum_{m=1}^{d} \frac{1}{m} \right)^2. \end{aligned} \tag{23}$$

For the sake of estimation, we will pretend that $\tilde{V}$ is a member of a GOE with width $\tilde{w}$.

Then, roughly, the degree of chaos in the magnetic field spectrum is determined by the ratio of $\tilde{w}$ to the mean level spacing in the magnetic field range of interest,

$$\frac{\tilde{w}}{1/\rho_B} = \frac{w}{\mu B_0} \frac{d+1}{2} \sum_{m=1}^{d} \frac{1}{m}. \tag{24}$$

The corresponding parameter determining the degree of chaos in the energy spectrum is $w/(1/\rho_E)$, where $\rho_E = E_0/d$ is the density of states for the energy levels. The relation between these two is therefore

$$\frac{\tilde{w}}{1/\rho_B} = \frac{w}{1/\rho_E} f_c(d), \tag{25}$$

where f_c is a correction function given by

$$f_c(d) = \frac{d+1}{2d} \sum_{m=1}^{d} \frac{1}{m}. \tag{26}$$

This factor is unity for $d = 1$, i.e., for no spin degeneracy. In this case the energy spectrum is just rescaled by the magnetic moment to become the magnetic field spectrum, and the Brody parameter ought therefore to come out the same. For nonzero spin degeneracy $d > 1$, however, $f_c > 1$, implying that the magnetic field spectrum should be *more chaotic* (larger Brody parameter) than the energy spectrum. This conclusion is restricted to the near-zero-field region $B \in [0, N_v B_0/d]$. In this region the density of states ρ_B grows rapidly as a function of degeneracy ($\sim d^2$), faster than the comparatively slow growth of the width parameter $\tilde{w} \sim \ln d/d$.

IV. CONCLUSIONS

In summary, we have verified, by numerical and semi-analytic considerations, that a molecule that exhibits partial chaos in its energy spectrum below its dissociation threshold, may appear to exhibit a greater degree of chaos as measured in its spectrum of Fano-Feshbach resonances. This conclusion, drawn from the nearest-neighbor-spacing distribution, is consistent with the general models of Ref. [1]. In both models the transition from the $B = 0$ energies to the $E = 0$ magnetic field resonance positions involves a series of avoided crossings, or alternatively, nontrivial magnetic moment fluctuations of the molecular states.

It is of course difficult to change the degree of chaos in a given molecule and to make a full study of the dependences in Figure 3. Nevertheless, the Dy_2 molecule as measured in Ref. [1] has Brody parameters ν_B somewhat less than unity. It is therefore conceivable that a measurement of the energy spectrum of Dy_2 at fixed magnetic field, for example by microwave spectroscopy, would be capable of testing the hypothesis that $\nu_E < \nu_B$ for this molecule. Effectively varying the degree of chaos native to a molecule may have to wait until similar spectra are measured in alternative, less chaotic molecules elsewhere in the periodic table.

Acknowledgements

We acknowledge useful discussions with J. d'Incao and M. Sze. We also acknowledge funding from the U.S.

Army Research Office under ARO Grant No. W911NF-12-1-0476 and from the JILA NSF Physics Frontier Center, PHY-1734006. L.D.A. acknowledges the financial support of the Czech Science Foundation (Grant Nos. P209/18-00918S and P208/17-26751Y).

[1] T. Maier, H. Kadau, M. Schmitt, M. Wenzel, I. Ferrier-Barbut, T. Pfau, A. Frisch, S. Baier, K. Aikawa, L. Chomaz, et al., Phys. Rev. X **5**, 041029 (2015).
[2] A. Frisch, M. Mark, K. Aikawa, F. Ferlaino, J. L. Bohn, C. Makrides, A. Petrov, and S. Kotochigova, Nature **507**, 475 (2014).
[3] T. Maier, I. Ferrier-Barbut, H. Kadau, M. Schmitt, M. Wenzel, C. Wink, T. Pfau, K. Jachymski, and P. S. Julienne, Phys. Rev. A **92**, 060702 (2015).
[4] K. Baumann, N. Q. Burdick, M. Lu, and B. L. Lev, Phys. Rev. A **89**, 020701 (2014).
[5] K. Aikawa, A. Frisch, M. Mark, S. Baier, A. Rietzler, R. Grimm, and F. Ferlaino, Phys. Rev. Lett. **108**, 210401 (2012).
[6] D. M. Leitner, R. S. Berry, and R. M. Whitnell, The Journal of Chemical Physics **91**, 3470 (1989).
[7] M. D. Frye, M. Morita, C. L. Vaillant, D. G. Green, and J. M. Hutson, Phys. Rev. A **93**, 052713 (2016).
[8] T. A. Brody, Lett. Nuovo Cimento **7**, 482 (1973).
[9] B. R. Judd and I. Lindgren, Phys. Rev. **122**, 1802 (1961).
[10] A. Petrov, E. Tiesinga, and S. Kotochigova, Phys. Rev. Lett. **109**, 103002 (2012).
[11] B. C. Yang, J. Pérez-Ríos, and F. Robicheaux, Phys. Rev. Lett. **118**, 154101 (2017).
[12] T. Maier, I. Ferrier-Barbut, H. Kadau, M. Schmitt, M. Wenzel, C. Wink, T. Pfau, K. Jachymski, and P. S. Julienne, Phys. Rev. A **92**, 060702 (2015).
[13] J. Mur-Petit and R. A. Molina, Phys. Rev. E **92**, 042906 (2015).
[14] R. A. Molina, J. Retamosa, L. Muiñoz, A. Relaño, and E. Faleiro, Physics Letters B **644**, 25 (2007).
[15] K. Życzkowski, M. Lewenstein, M. Kuś, and F. Izrailev, Phys. Rev. A **45**, 811 (1992).